

Quicker flocking in aligning active matters for noisier beginning

Sohini Chatterjee,* Sohom Das,* Purnendu Pathak,* Tanay Paul,* and Subir K. Das†

Theoretical Sciences Unit and School of Advanced Materials,

Jawaharlal Nehru Centre for Advanced Scientific Research, Jakkur, Bangalore 560064, India

(Dated: February 11, 2025)

The constituents in a class of active matter systems change their directions of motion by being influenced by the velocities of the neighbors. Such systems may undergo phase transitions, with respect to ordering in the velocity field, as well as clustering in the density field, when the strength of an externally imposed noise is varied. Via computer simulations, with a well-known model, that faithfully represents these systems, we show that evolutions in both clustering and ordering exhibit certain interesting features that were hitherto unrealized. The transformations occur quicker, following quenches to a fixed final state, below the transition point, for disordered starting states that are farther away from the “critical” noise strength. This implies earliest arrival of the farthest, at a given destination. Detailed analysis of the results, combined with the outcomes from a similar study of para- to ferromagnetic transitions, show that the variation in critical fluctuations in the initial configurations can lead to such interesting effect. We quantify this via the Ornstein-Zernike theory.

INTRODUCTION

Evolution towards a new state, following the quench of a homogeneous system inside the ordered or coexistence region of a phase diagram, is a complex dynamical process [1, 2]. Understanding of such kinetics of phase transitions is of much interest for passive as well as active matters [1, 3–11]. For the quenching experiments, traditionally one considers initial configurations that possess constituents having random directionalities or positions [8–23]. These correspond to states with insignificant spatial correlations [24]. However, it is important to carry out similar exercises with initial states of different varieties. Such practical protocol may lead to interesting outcomes when there exists interplay [25–29] between critical [2, 24] and coarsening phenomena [1–3]. In the long time (t) limit, it is of interest to see [25–29] if universal pictures emerge – whether the results remain same irrespective of the degree of spatial correlations at the starting configurations. Furthermore, it is important to investigate how the change in (steady-state) correlation, with the shift of the initial state towards a “critical” point, may affect the nature and alter

* Equal contributions

† Email of corresponding author: das@jncasr.ac.in

the longevity of the pre-asymptotic coarsening process [30]. Even if the asymptotic rate of growth remains unchanged, despite the variation in the starting states, there will be differences in overall evolution. Quantification and understanding of this bear much practical and fundamental relevance in vast varieties of physical, chemical as well as biological systems.

Here, for a type of active matter [7, 8, 31–33], we study kinetics of transitions in two different fields, viz., ordering in the velocity field and clustering in the density field. The aim is to investigate the change in the rates of evolutions with the variation of initial state. It appears that for both the fields the evolutions get slower as the initial state is chosen closer to the critical point of transition [24, 34]. In thermodynamic sense, this implies that the farthest arrives at a destination earliest, which is counter-intuitive [30, 35]. Similar effect, in the context of passive matter has become a topic of considerable interest [30, 35–65]. E.g., faster freezing of a hotter sample of liquid water [35], than a colder one, when quenched to a fixed subzero temperature, has drawn significant attention. In the latter case, recent studies suggest that metastability could be the reason behind the surprising outcome [37, 38, 52, 66]. Our study, in addition to identifying a counterpart in active matter phase transitions, provides further new insight that metastability is not a necessity for such observation [37, 66]. This conclusion is further strengthened by presenting similar results for para- to ferromagnetic (PF) transitions [41, 42]. The results from multiple types of transformations point towards the existence of universality that we quantify via the Ornstein-Zernike theory [34].

MODEL AND METHODS

We consider a model [31, 32, 67–69] which incorporates a dynamical alignment interaction amongst the constituent point-like active particles. These particles self-propel on off-lattice planes with constant speed v_0 . The model exhibits rich structural and dynamical features that arise from the competition between this alignment interaction and a random noise ζ , that plays role analogous to temperature (T) in the PF transition. While moving with a velocity $\vec{v}_j (= v_0 e^{i\theta_j})$, at time t , after a step of size Δt , a particle j can change its direction θ_j , being influenced by the average direction of motion of its neighboring particles, with an uncertainty due to ζ . Thus [31], $\theta_j(t + \Delta t) = \langle \theta(t) \rangle_{\mathcal{R}_j} + \zeta$, \mathcal{R}_j defining the neighborhood around the j -th particle, $\langle \theta(t) \rangle_{\mathcal{R}_j}$ being calculated as [32] $\langle \theta(t) \rangle_{\mathcal{R}_j} = \arg[\sum_{k \in \mathcal{R}_j} e^{i\theta_k(t)}]$. We treat ζ as a uniform random noise within $[-\eta/2, \eta/2]$, $\eta \in [0, 2\pi]$. The update of position \vec{r}_j , for particle j , is given by [31, 69] $\vec{r}_j(t + \Delta t) = \vec{r}_j(t) + \vec{v}_j(t + \Delta t)\Delta t$. We set $\Delta t = 1$. The transition from a disordered to a flocking state, in this model, to be referred to as the Vicsek Model (VM), below η_c , the critical noise strength, is characterized via the calculation of the order parameter [31] $v_a = N^{-1} |\sum_{j=1}^N e^{i\theta_j}|$, N being the total number of particles in a periodic box of size $L \times L$. The average value of v_a is expected to be finite in a flocking state, and vanishingly small in a disordered one.

For the magnetic transition we have performed Monte Carlo (MC) simulations with the Ising model (IM), having the Hamiltonian [2, 3, 70] $H = -J \sum_{\langle i,j \rangle} S_i S_j$, $S_{i(j)} (= \pm 1)$ being a spin or an atomic magnet sitting at a lattice site $i(j)$, with J being the strength of the interaction between two such nearest neighbors. For a thermodynamically large lattice size, i.e., for $L = \infty$, in space dimension $d = 2$, this model exhibits a phase transition [2, 3, 70] at the critical temperature $T_c \simeq 2.269J/k_B$, k_B being the Boltzmann constant. In our MC simulations, a trial move is made by randomly choosing a spin and altering its sign [70]. The move is accepted via the Metropolis algorithm [70]. L^2 such trials make a MC step (MCS), our time unit. For this model the equilibrium order parameter $m (= \sum_i S_i/L^2)$ is the magnetization per spin.

For the VM, alongside a transition in the velocity field, a flavor of vapor-liquid transition is also present. Such phase separation can be probed via the two-point equal-time correlation function [1] $C(r, t) = \langle \psi(\vec{r}, t) \psi(\vec{0}, t) \rangle - \langle \psi(\vec{r}, t) \rangle \langle \psi(\vec{0}, t) \rangle$; $r = |\vec{r}|$. Here $\psi(\vec{r}, t)$ is the local density-field order-parameter at time t at a space point \vec{r} on a lattice to which our off-lattice systems are mapped on, for the sake of convenience [71]. We have assigned $\psi = +1$ if the local density, computed within a circular region of unit radius around the point \vec{r} , is larger than the overall particle density, $\rho_0 = N/L^2$, otherwise -1 . Thus, for the analysis purpose, we have a picture analogous to the IM [72]. The enhancement of density inhomogeneity in a system can be quantified by extracting a length scale, $\ell(t)$, from the decay of $C(r, t)$ to a reference value C_{ref} , at different times. Analogously, depending upon the density, it may also be instructive to calculate average number of particles in (discrete) clusters after appropriate identification of the latter [9, 71] by setting an interparticle distance (d_c) criterion for particles belonging to a common cluster. Here we will present results for the largest clusters, as a function of time, which also is an important quantity. In this study, we have considered $\rho_0 = 0.5$, $v_0 = 0.03$, $C_{\text{ref}} = 0.1$ and $d_c = 1.5$. The choices for first two parameters provide [32] $\eta_c \simeq 1.5$, when $L = \infty$. Initial or starting configurations for the VM, with almost vanishing v_a , have been prepared by carrying out simulations at different η values, $\eta_s (> \eta_c)$, beginning with configurations having random assignments of both positions and velocities. The steady-state configurations, thus obtained, have been quenched to a fixed noise strength $\eta_f = 0.5$.

Each simulation box, for the VM, has been divided into square cells of unit side length. For a particle of interest, the alignment interaction range \mathcal{R} is defined as the cell in which the particle is located, along with its eight neighboring cells. Results are presented for systems of size $L = 256$, with $N = 32768$. The system size for the IM remains the same, containing 65536 spins. In this case, for the preparation of initial configurations we have chosen starting temperatures T_s above T_c . Configurations from there, with small m , are quenched to a final temperature $T_f = 0.5T_c$. Unless otherwise mentioned, all discussions are for the VM. The quantitative results correspond to statistics over 20000 initial configurations.

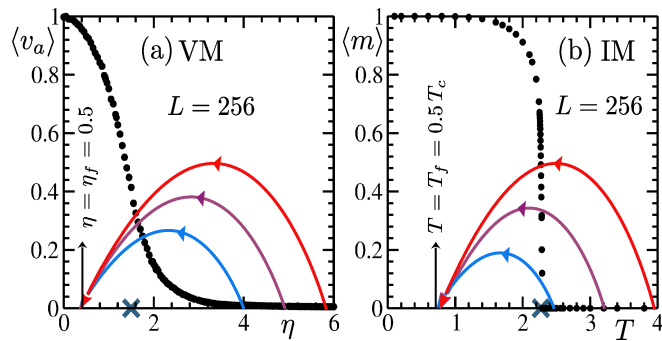


FIG. 1. (a) Average order parameter for the active matter model is plotted versus η . The protocol for quenches from different starting noise strengths, η_s , to a final strength, $\eta_f (= 0.5)$, has been sketched. (b) Same as (a) but here the phase diagram and the protocol (for quenches from different starting temperatures T_s to the specified T_f) are for the magnetic model. The critical points in the thermodynamic limit are marked by the crosses [24, 32].

RESULTS

In Fig. 1 (a) the symbols show a plot of the average order parameter, $\langle v_a \rangle$, versus η , for the VM. For each η , $\langle v_a \rangle$ was obtained by constructing distributions, via many simulations, starting with random initial configurations, over long times, in the respective steady state. The curved lines, with arrows, depict the protocol we have used for the investigation of the initial state dependence of coarsening that may lead to the effect discussed above. Analogous phase diagram, in magnetization versus T plane, along with the protocol, for the IM, is shown in Fig. 1 (b).

In Fig. 2 we show certain snapshots for the VM. The two upper frames contain representative steady-state pictures from two values of η_s . For the higher η_s , there exists more randomness in both positions and velocities. The lower frames display evolution snapshots that are obtained following quenches of the upper snapshots to $\eta_f = 0.5$. Clearly, both velocity ordering and density field clustering are occurring quicker for $\eta_s = 2\pi$, i.e., for the starting configuration that is farther from η_c . Note that for both the η_s , the snapshots are recorded at the same instant following the quenches. This difference in the pace of phase transitions is not only a fact corresponding to this particular combination of initial configurations, the trend is rather general.

In Fig. 3 (a) we show the average sizes of largest clusters, versus time, for three η_s . We have divided the results into two time regimes. The lower plots represent data from early times and the later time data are shown in the upper half of the broken frame. The orders of appearances of the data sets are different for very early and the later time regimes. Clearly, at late times the clusters are larger for higher starting noises. In the literature of phase-separation kinetics, it is, however, more customary to discuss the time dependence of ℓ . In Fig. 3 (b) we show ℓ versus t plots for the same set of η_s . This also conveys same surprising message.

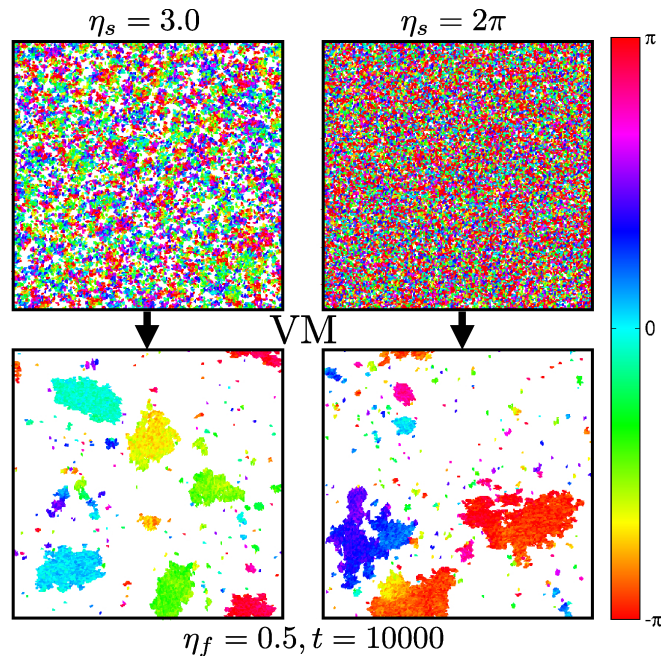


FIG. 2. Upper frames: Representative steady-state snapshots for two different values of η_s . Lower frames: Snapshots from $t = 10000$, taken during evolutions, following the quenches of the upper configurations to $\eta_f = 0.5$. The positions of the particles are marked. The color coding represents directionality of motion.

One may inquire whether there exists structural similarity during evolutions for all the considered values of η_s . To verify this, in Fig. 3 (c) we show the scaled correlation functions [1], the lower and upper sub-frames containing data from early and late times. Nice collapse of data from each η_s , upon scaling of the distance by corresponding ℓ , confirms the existence of structural similarity, though at somewhat late times.

For spin systems [41, 42], similar effect was argued to arise due to differences in spatial correlations in the initial states. With the intention of examining whether such a scenario applies here as well, we calculate the structure factor, $S(k) = \langle \psi_k \psi_{-k} \rangle$, ψ_k being the Fourier transform of $\psi(\vec{r})$, to estimate ξ , the correlation length, via the Ornstein-Zernike (OZ) relation $1/S(k) \propto (1 + k^2 \xi^2)$. In Fig. 4 (a) we show, for the VM, plots of $S(k)^{-1}$, versus k^2 . The trend, with the variation of η_s , reflects the fact that fluctuation becomes critical with the decrease of η_s . The linear appearances imply that the OZ behavior is obeyed. From the slopes we calculate ξ . In Fig. 4 (b) we show ξ , versus η_s . There we have also plotted IM data, versus T_s . Critical enhancements are very clear.

Next, we calculate the times, t_{c,η_r} , for crossings of the domain length plot for a reference value of $\eta_r = \eta_s = 2\pi$, the highest admissible noise within the model, with those for others. For the Ising case we represent the crossing times as t_{c,T_r} , with $T_r = \infty$, that corresponds to a perfectly random configuration. In Fig. 4 (c) we plot the corresponding results for both the

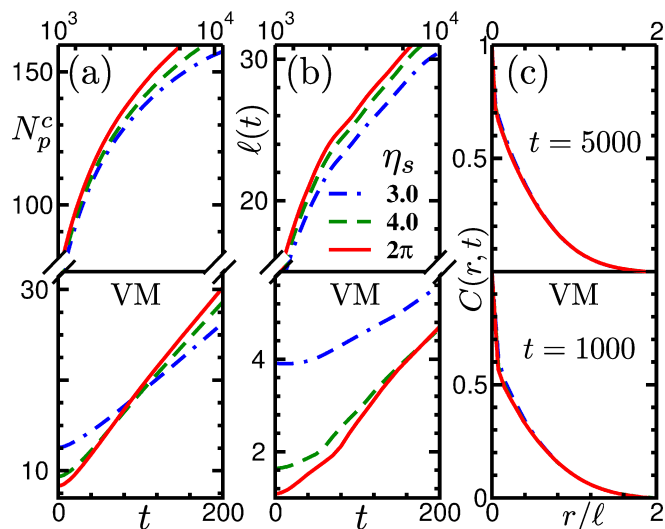


FIG. 3. (a) Plots of (averages of the) largest cluster sizes, related to the density field phase separation, versus time, for $\eta_s = 2\pi, 4.0$, and 3.0 . (b) Plots of the corresponding average domain lengths, versus time. (c) Scaling plots of two-point equal-time density correlation functions for the same set of η_s . The results correspond to $\eta_f = 0.5$.

models, versus ξ (at η_s or T_s). Nice (almost) linear scaling for both the models implies possible existence of a universal feature. Note that these plots also imply that systems with high initial noise or temperature eventually overtake all other systems starting with corresponding lower numbers.

All our presented results are obtained by averaging over runs with large number of independent initial configurations, to draw the conclusions carefully. Nevertheless, to further ascertain the correctness of these, given that the observation is counterintuitive, we have calculated the Pearson correlation coefficient, r_{t_c, η_s} , defined as [73] $r_{t_c, \eta_s} = \sum_{s=1}^n x_s y_s / [(\sum_{s=1}^n x_s^2)(\sum_{s=1}^n y_s^2)]^{1/2}$, where $x_s = t_{c, \eta_r}(\eta_s) - \bar{t}_{c, \eta_r}$ and $y_s = \eta_s - \bar{\eta}_s$, with \bar{t}_{c, η_r} and $\bar{\eta}_s$ being the average crossing time and the average noise strength, respectively, for a sample size $n = 3$, corresponding to $\eta_s = 2.5, 3, 4$. For this purpose, we have divided the full sets of initial configurations into 400 subsets. For each of these subsets, r_{t_c, η_s} is calculated. From these we have derived $P(r_{t_c, \eta_s})$, the probability distribution for r_{t_c, η_s} . The distribution for VM is shown in Fig. 4 (d). Quite clearly the peak appears very close to -1 , implying anticorrelations as clear likelihood. This is because higher randomness, in each small subset of initial configurations, leads to quicker clustering, i.e., the farthest arrives the earliest. The location of corresponding maximum for the IM is marked.

In the VM, the phase separation in the density field is supposed to be driven by the ordering in the velocity field. So, it is natural to ask: Should there be faster ordering as well for higher η_s ? This indeed is the case. See Fig. 5 (a). Here we plot $\langle v_a \rangle$, versus t , for several η_s . The growth there implies ordering, that occurs faster for higher η_s ! The reason should again

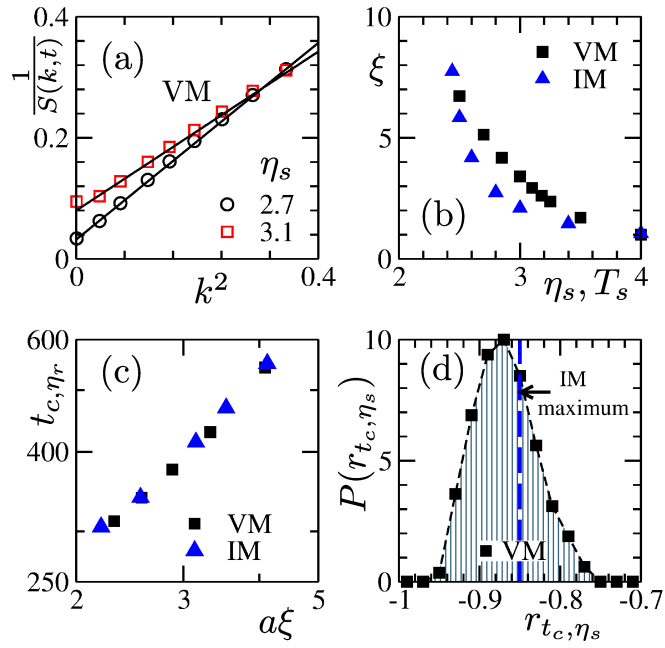


FIG. 4. (a) Plots of $1/S(k)$, versus k^2 , for two values of η_s . The continuous lines correspond to Ornstein-Zernike (OZ) expectation. (b) Correlation lengths ξ , calculated using the OZ relation, are plotted against η_s and T_s , respectively, for the VM and the IM. (c) Plots of crossing times t_{c, η_r} , versus ξ , for the VM and the IM. To compare the scaling for the two models, a prefactor a has been introduced in the abscissa. (d) Distribution of the Pearson correlation coefficient, r_{t_c, η_s} , for the VM. The location of the corresponding maximum for the IM has been shown by the dashed vertical line.

be related to fluctuation becoming critical with the approach of η_s to η_c . Because of voids, owing to clustering in the density field, we do not estimate correlation or domain lengths for the velocity field, rather look (see Fig. 5 (b)) at the susceptibility ($\chi = (\langle v_a^2 \rangle - \langle v_a \rangle^2)L^2$) as $\eta_s \rightarrow \eta_c$. Clearly, there is enhancement. Thus, for both the fields, the faster approach to new steady states are driven by the lack of critical fluctuation.

Finally, we define a quantity r_{v_a, η_s} , analogous to r_{t_c, η_s} . The exercise with r_{v_a, η_s} is simply to identify how steady the sequence of appearances of the plots is. For the calculated values of r_{v_a, η_s} , we have fixed $\langle v_a \rangle$ at 0.35. A distribution of this is shown in Fig. 5 (c). A message similar to Fig. 4 (d) clearly emerges, i.e., faster ordering for the farthest is quite general, not exhibited merely by a small fraction of initial configurations.

CONCLUSION

We have studied kinetics related to a class of active matter systems [31] that exhibit order-disorder transitions due to aligning dynamic interaction. As opposed to the traditional studies of coarsening phenomena [1, 3], we prepare disordered configurations

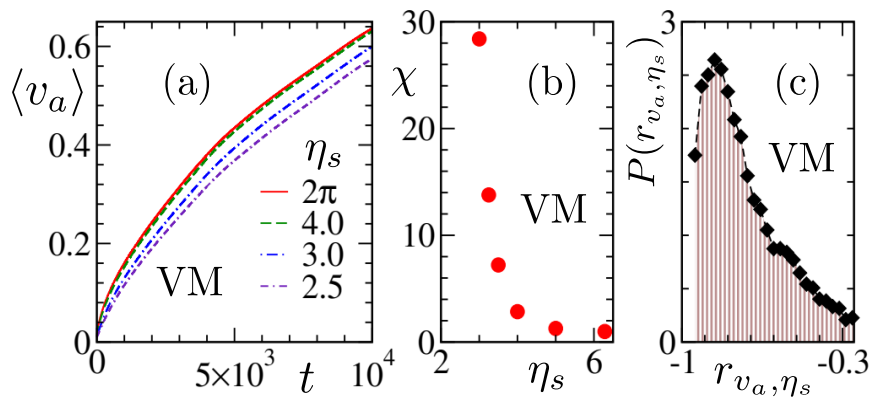


FIG. 5. (a) Average Vicsek order parameter, for a set of η_s , with the variation of time. (b) Susceptibility for the VM is plotted versus η_s . (c) Distribution of the Pearson correlation coefficient concerning the evolution of $\langle v_a \rangle$.

at initial states having different values of the noise strength, η , the driving parameter for the transitions [31]. Following quenches inside the ordered region, interestingly, we observe that configurations with higher values of η reach the new steady state quicker, implying fastest arrival of the farthest. This is counterintuitive. Via analysis using a critical-point theory [34] we show that differences in the extent of spatial correlations at initial states give rise to this puzzling effect.

It appears that certain relaxation time, associated with this effect, exhibits power-law scaling with the variation of initial correlation length. For a comparison we have presented similar results for model para- to ferromagnetic transitions [42] for which the transition is driven by the variation in temperature. Interestingly, similar scaling exists there as well, suggesting universality. This overall observation is analogous to the Mpemba effect [35] which is related to faster freezing of hotter water. It is believed that in water and several other systems the effect appears due to reasons connecting metastability [30, 37, 38, 40]. Contrary to this understanding, our work shows that metastability is not a necessary condition.

It should be noted that the enhancement in spatial correlation with approach to the transition point has counterparts in transitions in water and other materials [24, 34]. Thus, our work invites theoretical and experimental studies of coarsening dynamics in various other passive and active matters by preparing configurations at initial state points that lie along the critical loci, e.g., critical density line for water.

AUTHOR CONTRIBUTION

SKD proposed the project, designed the problem, supervised the work and wrote the manuscript. SC, SD and PP wrote the codes, carried out the simulations and performed the analyses. TP supervised the technical aspects, alongside writing codes and

producing representative results.

ACKNOWLEDGEMENT

The authors acknowledge computation times in the clusters of National Supercomputer Mission located in JNCASR.

-
- [1] A. J. Bray, Theory of Phase-Ordering Kinetics, *Adv. Phys.* **51**, 481 (2002).
- [2] A. Onuki, *Phase Transition Dynamics* (Cambridge University Press, Cambridge, UK, 2002).
- [3] S. Puri and V. Wadhawan, eds., *Kinetics of Phase Transitions* (CRC Press, Boca Raton, 2009).
- [4] J. Stenhammar, A. Tiribocchi, R. J. Allen, D. Marenduzzo, and M. E. Cates, Continuum Theory of Phase Separation Kinetics for Active Brownian Particles, *Phys. Rev. Lett.* **111**, 145702 (2013).
- [5] G. S. Redner, M. F. Hagan, and A. Baskaran, Structure and Dynamics of a Phase-Separating Active Colloidal Fluid, *Phys. Rev. Lett.* **110**, 055701 (2013).
- [6] S. Dey, D. Das, and R. Rajesh, Spatial Structures and Giant Number Fluctuations in Models of Active Matter, *Phys. Rev. Lett.* **108**, 238001 (2012).
- [7] S. K. Das, S. A. Egorov, B. Trefz, P. Virnau, and K. Binder, Phase Behavior of Active Swimmers in Depletants: Molecular Dynamics and Integral Equation Theory, *Phys. Rev. Lett.* **112**, 198301 (2014).
- [8] S. K. Das, Pattern, Growth, and Aging in Aggregation Kinetics of a Vicsek-like Active Matter Model, *J. Chem. Phys.* **146**, 044902 (2017).
- [9] S. Paul, A. Bera, and S. K. Das, How do clusters in Phase-Separating Active Matter Systems Grow? A Study for Vicsek Activity in Systems Undergoing Vapor–Solid Transition, *Soft Matter* **17**, 645 (2021).
- [10] N. Katyal, S. Dey, D. Das, and S. Puri, Coarsening Dynamics in the Vicsek Model of Active Matter, *Eur. Phys. J. E* **43**, 10 (2020).
- [11] T. Paul, N. Vadakkayil, and S. K. Das, Finite-Size Scaling in Kinetics of Phase Separation in Certain Models of Aligning Active Particles, *Phys. Rev. E* **109**, 064607 (2024).
- [12] P. Cremer and H. Löwen, Scaling of Cluster Growth for Coagulating Active Particles, *Phys. Rev. E* **89**, 022307 (2014).
- [13] F. Peruani and M. Baer, A Kinetic Model and Scaling Properties of Non-Equilibrium Clustering of Self-Propelled Particles, *New J. Phys.* **15**, 065009 (2013).
- [14] T. Surrey, F. Nédélec, S. Leibler, and E. Karsenti, Physical Properties Determining Self-Organization of Motors and Microtubules, *Science* **292**, 1167 (2001).
- [15] I. Buttinoni, J. Bialké, F. Kümmel, H. Löwen, C. Bechinger, and T. Speck, Dynamical Clustering and Phase Separation in Suspensions of Self-Propelled Colloidal Particles, *Phys. Rev. Lett.* **110**, 238301 (2013).

- [16] L. Huber, R. Suzuki, T. Krüger, E. Frey, and A. Bausch, Emergence of Coexisting Ordered States in Active Matter Systems, *Science* **361**, 255 (2018).
- [17] J. Grauer, F. Schmidt, J. Pineda, B. Midtvedt, H. Löwen, G. Volpe, and B. Liebchen, Active Droplids, *Nat. Commun.* **12**, 6005 (2021).
- [18] A. Bera, S. Sahoo, S. Thakur, and S. K. Das, Active Particles in Explicit Solvent: Dynamics of Clustering for Alignment Interaction, *Phys. Rev. E* **105**, 014606 (2022).
- [19] S. Mishra, S. Puri, and S. Ramaswamy, Aspects of the Density Field in an Active Nematic, *Philos. Trans. A: Math. Phys. Eng. Sci.* **372**, 20130364 (2014).
- [20] A. Parameshwaran and B. S. Gupta, Kinetics of Vapor-Liquid Transition of Active Matter System Under Quasi One-Dimensional Confinement, arXiv:2408.01195 (2024).
- [21] A. P. Solon, H. Chaté, and J. Tailleur, From Phase to Microphase Separation in Flocking Models: The Essential Role of Nonequilibrium Fluctuations, *Phys. Rev. Lett.* **114**, 068101 (2015).
- [22] S. Paul, S. Majumder, S. K. Das, and W. Janke, Effects of Alignment Activity on the Collapse Kinetics of a Flexible Polymer, *Soft Matter* **18**, 1978 (2022).
- [23] C. B. Caporusso, L. F. Cugliandolo, P. Digregorio, G. Gonnella, D. Levis, and A. Suma, Dynamics of Motility-Induced Clusters: Coarsening beyond Ostwald Ripening, *Phys. Rev. Lett.* **131**, 068201 (2023).
- [24] M. E. Fisher, The Theory of Equilibrium Critical Phenomena, *Rep. Prog. Phys.* **30**, 615 (1967).
- [25] A. J. Bray, K. Humayun, and T. J. Newman, Kinetics of Ordering for Correlated Initial Conditions, *Phys. Rev. B* **43**, 3699 (1991).
- [26] T. Blanchard, L. F. Cugliandolo, and M. Picco, Persistence in the Two Dimensional Ferromagnetic Ising Model, *J. Stat. Mech: Theor. Expt.* **2014**, P12021 (2014).
- [27] S. Chakraborty and S. K. Das, Role of Initial Correlation in Coarsening of a Ferromagnet, *Eur. Phys. J. B* **88**, 160 (2015).
- [28] S. K. Das, K. Das, N. Vadakkayil, S. Chakraborty, and S. Paul, Initial Correlation Dependence of Aging in Phase Separating Solid Binary Mixtures and Ordering Ferromagnets, *J. Phys. Condens. Matter* **32**, 184005 (2020).
- [29] K. Das, N. Vadakkayil, and S. K. Das, Aging Exponents for Nonequilibrium Dynamics Following Quenches from Critical Points, *Phys. Rev. E* **101**, 062112 (2020).
- [30] S. K. Das, Perspectives on Certain Puzzles in Phase Transformations: When Should the Farthest Reach the Earliest?, *Langmuir* **39**, 10715 (2023).
- [31] T. Vicsek, A. Czirók, E. Ben-Jacob, I. Cohen, and O. Shochet, Novel Type of Phase Transition in a System of Self-Driven Particles, *Phys. Rev. Lett.* **75**, 1226 (1995).
- [32] A. Czirók, H. E. Stanley, and T. Vicsek, Spontaneously Ordered Motion of Self-Propelled Particles, *J. Phys. A Math. Gen.* **30**, 1375 (1997).
- [33] T. Vicsek and A. Zafeiris, Collective Motion, *Phys. Rep.* **517**, 71 (2012).
- [34] H. E. Stanley, *Introduction to Phase Transitions and Critical Phenomena* (Clarendon Press, Oxford, 1971).

- [35] E. B. Mpemba and D. G. Osborne, Cool?, *Physics Education* **4**, 172 (1969).
- [36] Aristotle, *Meteorologica*, edited by H. D. Lee (Harvard University Press, Cambridge, 1962).
- [37] S. Ghosh, P. Pathak, S. Chatterjee, and S. K. Das, Simulations of Mpemba Effect in WATER, Lennard-Jones and Ising Models: Metastability vs Critical Fluctuations, arXiv:2407.06954v1 (2024).
- [38] J. Bechhoefer, A. Kumar, and R. Chérite, A Fresh Understanding of the Mpemba Effect, *Nat. Rev. Phys.* **3**, 534 (2021).
- [39] M. Jeng, The Mpemba Effect: When Can Hot Water Freeze Faster Than Cold?, *Am. J. Phys.* **74**, 514 (2006).
- [40] M. Baity-Jesi et. al., The Mpemba Effect in Spin Glasses is a Persistent Memory Effect, *Proc. Natl. Acad. Sci. U. S. A.* **116**, 15350 (2019).
- [41] N. Vadakkayil and S. K. Das, Should a Hotter Paramagnet Transform Quicker To a Ferromagnet? Monte Carlo Simulation Results for Ising Model, *Phys. Chem. Chem. Phys.* **23**, 11186 (2021).
- [42] S. Chatterjee, S. Ghosh, N. Vadakkayil, T. Paul, S. K. Singha, and S. K. Das, Mpemba effect in Pure Spin Systems : A Universal Picture of the Role of Spatial Correlations at Initial States, *Phys. Rev. E* **110**, L012103 (2024).
- [43] A. Gal and O. Raz, Precooling Strategy Allows Exponentially Faster Heating, *Phys. Rev. Lett.* **124**, 060602 (2020).
- [44] P. Chaddah, S. Dash, K. Kumar, and A. Banerjee, Overtaking while Approaching Equilibrium, arXiv:1011.3598 (2010).
- [45] A. Kumar and J. Bechhoefer, Exponentially Faster Cooling in a Colloidal System, *Nature* **584**, 64 (2020).
- [46] R. Chérite, A. Kumar, and J. Bechhoefer, The Metastable Mpemba Effect Corresponds to a Non-monotonic Temperature Dependence of Extractable Work, *Front. Phys.* **30**, 654271 (2021).
- [47] A. Lasanta, F. Vega Reyes, A. Prados, and A. Santos, When the Hotter Cools More Quickly: Mpemba Effect in Granular Fluids, *Phys. Rev. Lett.* **119**, 148001 (2017).
- [48] A. Torrente, M. A. López-Castaño, A. Lasanta, F. V. Reyes, A. Prados, and A. Santos, Large Mpemba-like effect in a Gas of Inelastic Rough Hard Spheres, *Phys. Rev. E* **99**, 060901 (2019).
- [49] E. Mompó, M. López-Castaño, A. Torrente, F. V. Reyes, and A. Lasanta, Memory Effects in a Gas of Viscoelastic Particles, *Physics of Fluids* **33**, 062005 (2021).
- [50] A. Biswas, V. V. Prasad, O. Raz, and R. Rajesh, Mpemba Effect in Driven Granular Maxwell Gases, *Phys. Rev. E* **102**, 012906 (2020).
- [51] A. Biswas, V. V. Prasad, and R. Rajesh, Mpemba Effect in Anisotropically Driven Inelastic Maxwell Gases, *J. Stat. Phys.* **186**, 45 (2022).
- [52] J. Jin and W. A. I. Goddard, Mechanisms Underlying the Mpemba Effect in Water from Molecular Dynamics Simulations, *J. Phys. Chem. C* **119**, 2622 (2015).
- [53] Y. Tao, W. Zou, J. Jia, W. Li, and D. Cremer, Different Ways of Hydrogen Bonding in Water - Why Does Warm Water Freeze Faster than Cold Water?, *J. Chem. Theory Comput* **13**, 55 (2017).
- [54] H. C. Burrige and P. F. Linden, Questioning the Mpemba Effect: Hot Water Does Not Cool More Quickly Than Cold, *Sci. Rep.* **6**, 37665 (2016).
- [55] Z. Lu and O. Raz, Nonequilibrium Thermodynamics of the Markovian Mpemba Effect and its Inverse, *Proc. Natl. Acad. Sci. U. S. A.* **114**, 5083 (2017).

- [56] I. Klich, O. Raz, O. Hirschberg, and M. Vucelja, Mpemba Index and Anomalous Relaxation, *Phys. Rev. X* **9**, 021060 (2019).
- [57] D. Auerbach, Supercooling and the Mpemba Effect: When Hot Water Freezes Quicker Than Cold, *Am. J. Phys.* **63**, 882 (1995).
- [58] M. Vynnycky and S. Kimura, Can Natural Convection Alone Explain the Mpemba Effect?, *Int. J. Heat Mass Transf.* **80**, 243 (2015).
- [59] X. Zhang, Y. Huang, Z. Ma, Y. Zhou, J. Zhou, W. Zheng, Q. Jiang, and C. Q. Sun, Hydrogen-bond Memory and Water-skin Supersolidity Resolving the Mpemba Paradox, *Phys. Chem. Chem. Phys.* **16**, 22995 (2014).
- [60] Z. Tang, W. Huang, Y. Zhang, Y. Liu, and L. Zhao, Direct Observation of the Mpemba Effect with Water: Probe the Mysterious Heat Transfer, *InfoMat* **5**, e12352 (2023).
- [61] F. J. Schwarzendahl and H. Löwen, Anomalous Cooling and Overcooling of Active Colloids, *Phys. Rev. Lett.* **129**, 138002 (2022).
- [62] Y. H. Ahn, H. Kang, D. Y. Koh, and H. Lee, Experimental Verifications of Mpemba-Like Behaviors of Clathrate Hydrates, *Korean J. Chem. Eng.* **33**, 1903 (2016).
- [63] P. A. Greaney, G. Lani, G. Cicero, and J. C. Grossman, Mpemba-Like Behavior in Carbon Nanotube Resonators, *Metall. Mater. Trans. A* **42**, 3907 (2011).
- [64] I. González-Adalid Pemartín, E. Mompó, A. Lasanta, V. Martín-Mayor, and J. Salas, Slow Growth of Magnetic Domains Helps Fast Evolution Routes for Out-of-Equilibrium Dynamics, *Phys. Rev. E* **104**, 044114 (2021).
- [65] A. K. Chatterjee, S. Takada, and H. Hayakawa, Quantum Mpemba Effect in a Quantum Dot with Reservoirs, *Phys. Rev. Lett.* **131**, 080402 (2023).
- [66] A. Biswas, R. Rajesh, and A. Pal, Mpemba effect in a Langevin system: Population Statistics, Metastability, and other Exact Results, *J. Chem. Phys.* **159**, 4 (2023).
- [67] G. Grégoire and H. Chaté, Onset of Collective and Cohesive Motion, *Phys. Rev. Lett.* **92**, 025702 (2004).
- [68] G. Baglietto and E. V. Albano, Finite-size Scaling Analysis and Dynamic Study of the Critical Behavior of a Model for the Collective Displacement of Self-driven Individuals, *Phys. Rev. E* **78**, 021125 (2008).
- [69] G. Baglietto and E. V. Albano, Nature of the Order-Disorder Transition in the Vicsek Model for the Collective Motion of Self-Propelled Particles, *Phys. Rev. E* **80**, 050103 (2009).
- [70] D. P. Landau and K. Binder, *A Guide to Monte Carlo Simulations in Statistical Physics* (Cambridge University Press, Cambridge, 2009).
- [71] S. Roy and S. K. Das, Dynamics and Growth of Droplets Close to the Two-Phase Coexistence Curve in Fluids, *Soft Matter* **9**, 4178 (2013).
- [72] S. Majumder and S. K. Das, Diffusive Domain Coarsening: Early Time Dynamics and Finite-size Effects, *Phys. Rev. E* **84**, 021110 (2011).
- [73] K. Pearson and F. Galton, Note on Regression and Inheritance in the Case of Two Parents, *Proc. R. Soc. Lond.* **58**, 240 (1895).